Int J Adv Manuf Technol (2017) 93:3203–3210
DOI 10.1007/s00170-017-0773-4

ORIGINAL ARTICLE

Experimental study of fibre laser microdrilling of aerospace superalloy by trepanning technique

F. Tagliaferri[1] · **S. Genna**[2] · **C. Leone**[2,3] · **B. Palumbo**[1] · **G. De Chiara**[4]

Received: 10 May 2017 / Accepted: 30 June 2017 / Published online: 14 July 2017

Abstract In the present study, fibre laser microdrilling of NIMONIC®263 sheet is investigated through an experimental testing campaign. Design of experiments (DOE) and analysis of variance (ANOVA) are applied with the aim to study the influence of the process parameters on the hole geometry and metallurgical properties. The results show that the laser allows drilling ~0.4-mm-thick NIMONIC®263 sheets with a trepanning speed up to 600 mm/min, obtaining good tolerance, low recast layer and absence of microcracks.

Keywords Nimonic · C263 · Recast layer · Effusion cooling system

1 Introduction

Nowadays, the development of higher-efficiency aero-engines involves the increasing of the flame temperature. The latter allows a reduction of the emission levels and the pressure losses. However, the increase of flame temperature is limited by the maximum temperature of the materials available for the engine construction [1]. To protect the combustor component from the hot temperature, it is possible to form a cooling film of air on the surface of the component, using of a large number of small holes (typically less than 1.0 mm in diameter) [2, 3]. Thus, in the hot section of aero-engines, an effusion cooling system is placed inside the turbine blade, allowing reducing thermal stress and avoiding premature failure of the turbine blades [3]. The turbine blade effusion system consists of a thin sheet, with more than 200 of neighbouring holes; the latter allows obtaining a cooling film within the blade wall. The holes diameters vary in the range of 0.3–1.0 mm.

Currently, electrical discharge machining (EDM) technique is adopted to drill the holes for effusion cooling systems of turbine blades in the hot section of aero-engines to satisfy the hole requirements (tight tolerances, no cracks in the base material and low recast layer). On the other hand, EDM microdrilling needs long process time and adopts dielectric liquid in which the workpiece is immersed. This liquid is not environment-friendly and needs to be processed.

Laser beam machining (LBM) represents a possible solution [4–10]. Compared to traditional technologies, laser drilling offers several benefits (i.e. absence of mechanical contact and tool wear reduction of liquid pollutants, no need for complex fixtures, high productivity, process flexibility and the possibility to create complex shapes and accurate geometries with narrow kerfs) on almost all categories of materials including metals [11–16], non-metals [17], ceramics [18] and composites [19].

In this research work, laser microdrilling of NIMONIC®263 sheets, 0.38 mm in thickness, by a 100 W fibre laser, working in modulated wave mode, is investigated. Two experimental test series were carried out. At first, pre-tests were executed varying the speed in the range 500–1000 mm/min, in order to identify a speed compatible with the machine dynamic. On the basis of the tests' results, and on the results of previous studies [20, 21], the control factor and their levels were individuated. In the second

✉ F. Tagliaferri
flaviana.tagliaferri@unina.it

1 Department of Industrial Engineering, University of Naples Federico II, P.le Tecchio 80, 80125 Naples, Italy

2 CIRTIBS Research Centre, University of Naples Federico II, P.le Tecchio 80, 80125 Naples, Italy

3 Department of Industrial and Information Engineering, University of Campania Luigi Vanvitelli, Via Roma 29 (Ce), 81031 Aversa, Italy

4 Avio Aero, Viale Giuseppe Luraghi 20, 80038 Pomigliano d'Arco, NA, Italy

Table 1 Main laser system characteristics (SPI-RedPower SP100C)

Parameters	Value	Unit
Wavelength	1090	[nm]
Maximum power	100	[W]
Mode operation	CW or modulated	–
Pulse frequency	1–18	[kHz][a]
Pulse duration	1–0.01 ms	[ms][a]
Beam diameter ($1/e^2$)	5.0 ± 0.5	[mm]
Full angle divergence	<0.4	[mrad]
Beam quality	TEM_{00} ($M^2 < 1.1$) BPP 0.38	– [mm.mrad]
Focal length	50	[mm]
Beam diameter at the focal spot	≈48	[μm]
Nozzle diameter	0.5	[mm]

[a] In modulated regime

experimental test series, drilling tests were performed by varying the speed, the pulse duration, the focus position and the tool path. The obtained holes were investigated by digital microscopy (KH-8700 by Hirox). The hole diameter and circularity were measured at the entrance and the exit of the laser beam.

Table 2 Chemical composition and properties of NIMONIC®263

Element	Ni	Co	Cr	Mo	Ti	C
Min [%]	Bal.	19	19	5.6	1.9	0.04
Max [%]		21	21	6.1	2.4	0.08
Element	Mn	Al	Si	Cu	Fe	S
Min [%]	–	–	–	–	–	
Max [%]	0.60	0.60	0.4	0.20	0.07	0.007
Element	B	Pb	Ag	Bi		
Min [%]	–	–	–	–		
Max [%]	0.005	0.002	0.0005	0.0001		
Physical properties			Value		Units	
Density			8.36		[g/cm^3]	
Melting Range						
Liquidus temperature			1355		[°C]	
Solidus temperature			1300			
Specific heat			461		[J/kg,°C]	
Thermal conductivity			11.72[a]		[W/m°C]	
Linear thermal expansion			11.0		[10^{-6}/°C]	
Mechanical properties[a]			Value		Units	
Tensile strength			1004[b]		[MPa]	
Yeld strength (at 0.2%)			585[b]		[MPa]	
Elongation			45[b]		[%]	
Reduction of area			41[b]		[%]	
Young's modulus			221[b]		[GPa]	
Torsional modulus			86[b]		[GPa]	

[a] Heat treatment: 2 h/1150 °C/WQ + 8 h/800 °C/AC

[b] At 20 °C

Table 3 Control factors and setting levels

Control factor	Low (−1)	Middle (0)	High (+1)	Unit
Pulse duration, *D*	0.1	0.2	0.4	[ms]
Speed, *S*	200	400	600	[mm/min]
Focus position, *F*	0	–	0.2	[mm]
Tool path, *Tp*	TP1	-	TP2	-

Analysis of variance (ANOVA) was adopted to study the influence of the process parameters on the hole characteristics.

2 Equipment, material and experimental procedures

A fibre laser (RedPower SP100C by SPI), working at the wavelength, $\lambda = 1090$ nm, was adopted for the drilling tests. In this device, the laser radiation is transferred via an optical fibre to the laser head (by HAAS LTI), that is mounted in a 3 + 1 axis CNC system, finecut (Y 340 M by ROFIN). An external laser controller (MCA LCT3001) controls the power (from 10 to 100% maximum nominal power) and the regime (continuous wave or modulated). In modulated regime, the pulse frequency and the pulse duration are settable by the controller. The CNC system controls the laser source power, the geometric patterns and the beam speed. Table 1 shows the main laser system characteristics.

The material used in the present investigation is NIMONIC®263, under form of rolled sheets, 0.38 mm in thickness, (UNS N07263/W. Nr. 2.4650). The NIMONIC® alloy 263 has high properties in terms of creep strength and stress. Table 2 shows the chemical composition and the main properties of NIMONIC®263 alloy.

The tests companion was developed adopting a systematic approach to design experiments, as proposed in [22] and successfully applied in [19–21, 23–26]. Pre-design sheets were developed on the basis of main bibliography [5–15], relevant background [20, 21] and pre-tests.

On the basis of bibliographic data [6], two laser-drilling techniques were considered: percussion drilling and trepanning drilling. Although percussion drilling has the potential for faster drilling times, trepanning generally gives better hole quality compared to the first one. On the other hand, trepanning drilling requires high quality beam (i.e. narrow beam with low M^2 factor). Consequently, it was chosen to adopt the latter technique together to a high brilliance laser source. The experimental campaign was developed in two steps. First, in order to find out a good level range for machining speed in trepanning drilling, pre-tests were performed. During this phase, the other process parameters were fixed according to

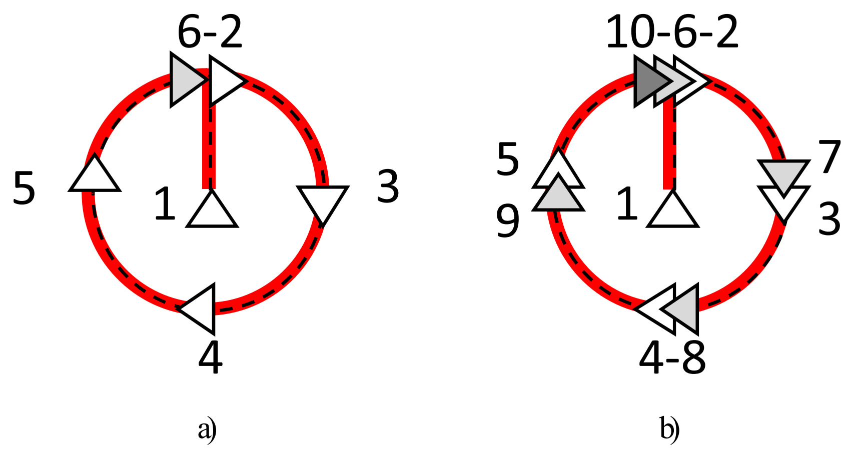

Fig. 1 Tool path for trepanning. **a** TP1. **b** TP2. In the figure, the *arrows* and the *numbers* indicate the path sequences

the value reported in Table 3. The speed values were identified on the basis of previous research [20, 21].

The chosen tool path (TP1) for the present tests was as follow: first the laser generates an initial hole (piercing), smaller than intended, at the centre of required location. After piercing, the laser beam moves along the radius and then to an orbit describing a circular path, to create the final hole (see Fig. 1a).

To study the influence of the control factors (i.e. laser parameters) on the hole characteristics, a second set of tests was performed, starting from the information came out from the preliminary tests. In this second phase, following to the design of experiments (DOE) methodology, a factorial plan was adopted.

The adopted control factors were pulse duration *D*, speed *S* focus position *F*, and tool path, *Tp*. The chosen tool paths for second test campaign were as follow: first, piercing in the middle of the area where the hole is to be produced, then the laser beam moves one time (TP1) or two time (TP2) through an orbit describing a circular path to create the final hole (see Fig. 1a, b).

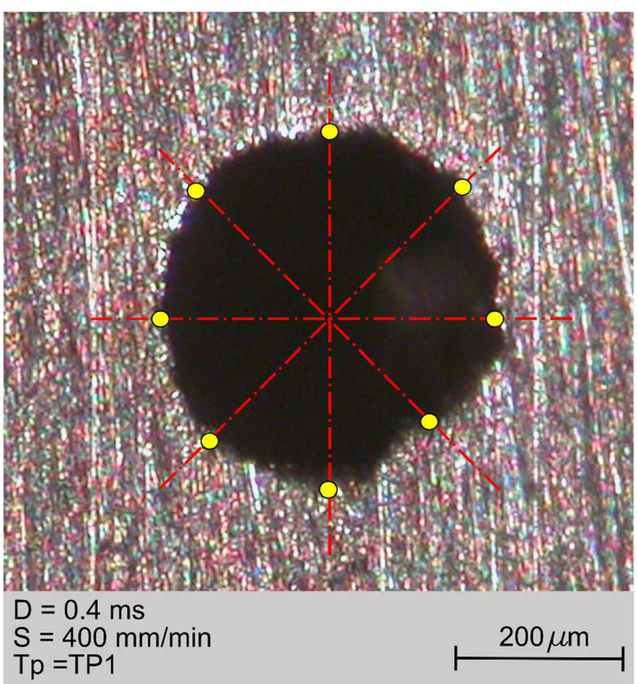

Fig. 2 Strategy for measuring with eight sectors

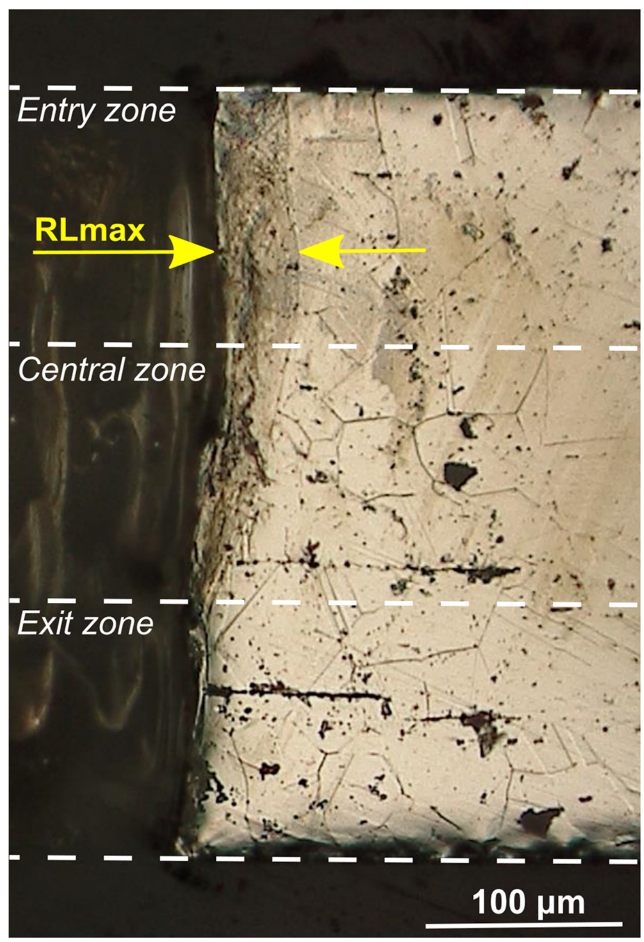

Fig. 3 Schematic of recast layer (RLmax) measurement

Table 4 Result of ANOVA in terms of *p* value

Source	Hole diameter at the entry (DEn)	Hole diameter at the exit section (DEx)	Hole circularity at the entry section (CEn)	Hole circularity at the exit section (CEx)	Recast layer (RLmax)	Taper angle (Ta)
D (pulse duration)	*0.012*	0.141	0.687	0.843	0.592	0.474
S (speed)	*0.000*	*0.001*	0.315	0.272	0.453	0.214
F (focus position)	0.174	0.361	0.938	0.649	0.281	0.783
Tp (Tool path)	0.994	0.866	0.334	0.504	0.589	0.746
D*S	0.119	0.267	*0.031*	*0.014*	0.196	0.120
D*F	0.193	0.393	0.449	0.368	0.756	0.068
D*Tp	0.452	0.923	0.864	0.732	0.806	0.732
S*F	0.330	0.358	0.216	0.202	0.802	0.777
S*Tp	0.552	0.910	0.072	0.631	0.426	0.180
F*Tp	0.161	0.813	0.529	0.888	0.417	0.465

The significant control factors (p value < 0.05) are italicized

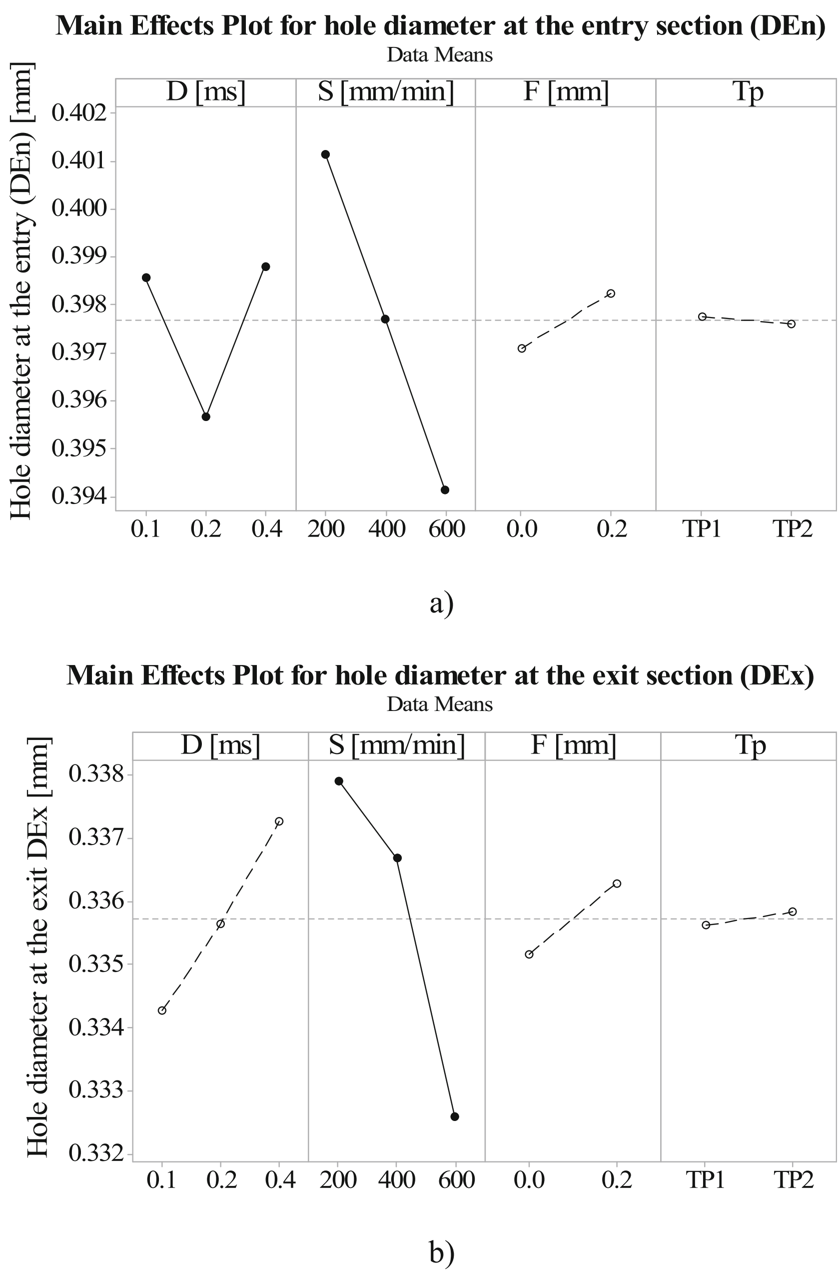

Fig. 4 Main effects plots for diameters at the **a** entry section (DEn) and **b** exit section (DEx)

Table 3 summarizes the control factors and their settings levels, adopted in the experimental phase. A full factorial experimental design was performed.

Each treatment (i.e. process condition) was repeated four times (four replications). Thus, a total of 144 experimental runs were performed. The replications of each treatment were executed in order to provide more consistent response repeatability during the first experimental study.

The order of trials was completely randomized (treatments and replications) to reduce the disturbance of any unconsidered noise factor.

The response variables considered for this study are the diameters of the entry (DEn) and exit (DEx) sections of the hole; the circularity of the hole for the entry (CEn) and exit (CEx) sections; recast layers (RLmax); and taper angle (Ta). Moreover, the presence of cracks and oxides were also checked.

According with ISO 12181-1:2011 (Geometrical product specifications—GPS—Roundness, which define the diameter as a parameter associated with a circle), the measuring was developed through an internal algorithm to detection system Quadracheck200 in combination to the microscope Stemi 2000CS. LSBF: Fit determined by minimizing the sum of the squared point deviation from the form fit.

The measuring procedure requires a minimum of three points to measure a circle, and a maximum of 100 points can be probed and will be processed by a fit algorithm to define the circle. So, in order to standardize the measurement procedure, removing the uncertainty connected to the operator, and reduce the measure time, a subdivision into eight sectors was used, as shown in Fig. 2. The eight points, in the intersection between the hole border and the sector pattern, were used for the hole fitting. The use of eight points was considered a good compromise in term of accuracy and measure time. Finally, the circularity at the entry and exit section was calculated as the ratio between the minimum inscribed and the maximum circumscribed diameters.

After the hole characteristic measurement, the specimens were embedded with an epoxy resin and then polished, using abrasive paper up to a grit size of P2500 (Standard ISO 6344). The recast layer extension was measured in three zones: at the entry, in the central, and at the exit section. The greatest value (worst condition) was adopted for the analysis. Figure 3 depicts a schematic of recast layer measurement.

3 Experimental results and discussion

All the 144 samples have never presented cracks, neither in the base material nor in the recast layer. This result is due to two reasons: in comparison with other superalloys (e.g. Inconel 718), the investigated material is less prone to crack formation. Moreover, the adopted average power and pulse power are very limited (80 and 100 W); thus, no large thermal shock occurs. This represents a fundamental result for the experimentation. In fact, the aeronautical restrictions require total absence for the cracks in the base material, since, as well known, they represent points of weakness in the final component.

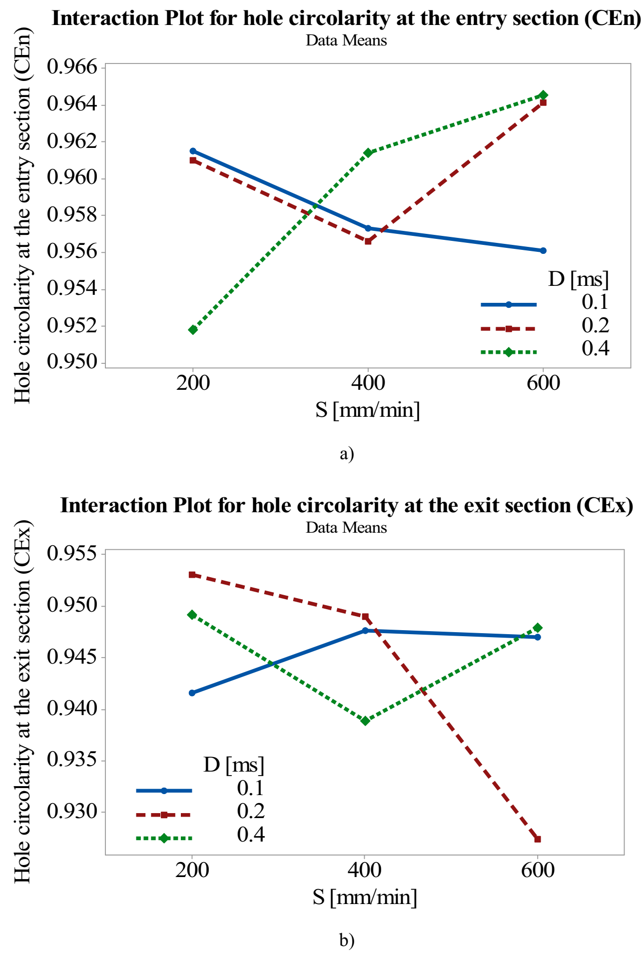

Fig. 5 Interaction plots for circularity of the hole at **a** the entry section (CEn) and **b** exit section (CEx)

In addition, the metallurgical analysis gave a total absence of oxides. This result was possible thanks to the use of an inert assistant gas (Nitrogen) during processing. However, it is necessary to specify that the use of such gas was effective because of the little thickness of the machined workpiece.

Table 5 Optimal parameter set

Control factor	Best set	Unit
Pulse duration, *D*	0.4	[ms]
Speed, *S*	600	[mm/min]
Focus position, *F*	0.2	[mm]
Tool path, *Tp*	TP1	–

Regarding the recast layer, it was found that about 65% of the treatments results into the aeronautical specification (thickness of recast layer less than 0.040 mm).

The ANOVA was used to check the statistical significance of the factor effects for each response variable. Before the analysis, the assumptions that the observations are normally and independently distributed were successfully checked via analysis of residuals, in agreement with [27]. Table 4 shows the ANOVA results, in terms of p values, for the studied response variables. Assuming a 95% confidence level ($\alpha = 0.05$), a control factor, or a combination of control factors, is considered significant where the p value is less than 0.05.

From Table 4, the DEn is affected by pulse duration (D) and speed (S); the DEx is affected by S, and the circularity (for both entry, Cen, and exit sections, CEx) is affected by interaction between pulse D and S. The ANOVA does not show any significant effect for RLmax and Ta. Figure 4a, b shows the main effect plots for the diameters of the entry and exit sections of the hole, respectively. The significant effects are drawn by continues lines. Figure 5 shows the significant interaction plots of circularity for the exit section.

Figure 4a depicts the main effects plot for DEn; this diameter has a minimum when the middle value of D is adopted ($D = 0.2$ ms). This phenomenon was not expected. Generally speaking, when higher pulse duration is adopted, a longer interaction time occurs; therefore, an increase of the diameter is expected, as reported in [28]. It is worth noting that the adopted laser source works in modulated regime; thus, to ensure a constant average power (80 W), when the pulse duration is low ($D = 0.1$ ms), the pulse frequency is high ($F = 8$ kHz). The opposite occurs when the duration is high ($D = 0.4$ m and $F = 2$ kHz). Therefore, it is possible to assume that the behaviour of the DEn is the result of two competing effects: the pulse width (which increases diameter) and the frequency (which decreases diameter).

Regarding the effect of the S on DEn, the behaviour shown in Fig. 4a is in accordance with the literature [10, 16, 29–31]: for a fixed average power, an increase in speed reduces the amount of energy released per unit length and thus the amount of removed material.

Similar remarks can be made on DEx, it decreases when the S increases (Fig. 4b).

Generally speaking, high speed values ensure low processing time, but results in low hole quality, either for the spot overlap decreasing and either for the increase of the vibrations on the laser machine. On the other hand, a too low speed gives a longer interaction between laser beam and workpiece, increasing the recast layer thickness inside the hole.

Regarding circularity, ANOVA does not indicate as significant any main effect, while marks as significant the interactions between speed and pulse duration (D*S). The first phenomenon can be explained taking into account the high levels of spot overlap: for all combinations of the control factors, the overlap is always higher than 90%. For this reason, the double orbitation (TP2) of the laser beam does not lead to an improvement of the circularity. The single orbitation (TP1) already guarantees an excellent finish in the contouring.

The statistically significant interaction plots are reported in Fig. 5. Figure 5a shows that the increasing of the S can produce opposite behaviours: when low level of pulse duration ($D = 0.1$ ms) is adopted, the circularity decreases; for high value of pulse duration ($D = 0.4$ ms), the circularity increases. This because, at low value of speed ($S = 200$ mm/min), high duration generates high molten material, that is hard to remove and so a highly irregular hole with low circularity is obtained.

On the contrary, low pulse D generates a lower quantity of molten that can be easily expelled, allowing obtaining a more regular hole. When the speed increases ($S = 600$ mm/min), the opposite occurs: the increase of speed creates a benefit when the pulse duration is high, because less molten material is generated for the reductions of the interaction time, and so a more regular hole is obtained.

Figure 5b shows the interactions between D*S for CEx. The statistical significance of this interaction is marked because of the strong decrease of CEx when the intermediate value of pulse duration ($D = 0.2$) is adopted. Such behaviour could be in line with the pulse on and pulse off mechanism:

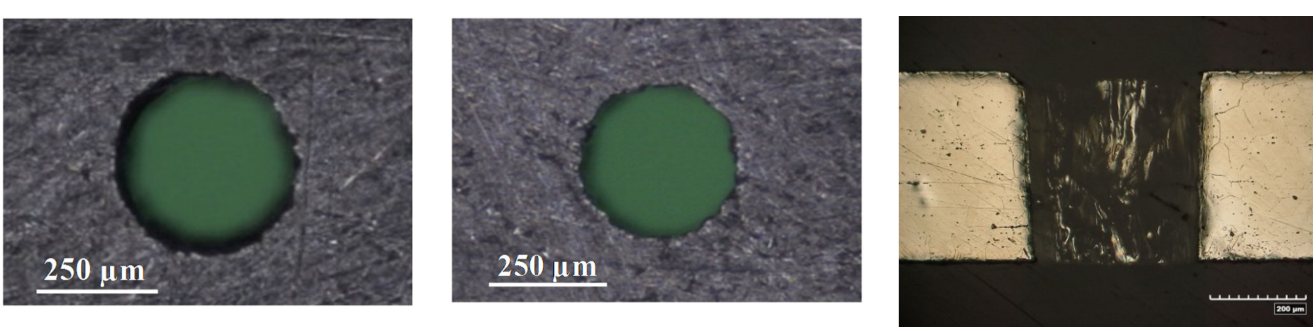

a) b) c)

Fig. 6 Hole aspect at **a** entry, **b** exit, and **c** cross section obtained with the optimal parameter set when the pulse *D* is set at 0.2 ms, the molten material is not so hot, and therefore, an increase of the speed can only worsen the contouring mechanism, giving a lower circularity in exit.

As a result of the information came out from the analysis of both geometric and metallurgical data, it was possible to identify an optimal parameter set for the microdrilling process. The best parameter set are detailed in Table 5. Through this parameter set, the supposed time to complete the process for the whole component is around 10 min instead of about 120 min for the correspondent process by EDM. Figure 6 shows a hole obtained with the optimal parameter set.

4 Conclusion

In this study, laser microdrilling of NIMONIC®263 sheet was performed by modulated fibre laser, to study how the process parameters affect the quality of the holes. On the basis of the discussed results, the main conclusions can be summarized as follow:

- fibre laser technology represents a valid alternative to EDM technology in the processing of the effusion cooling systems, ensuring a good quality and lower processing time;
- all the holes are free from cracks, neither in the base material nor in the recast layer;
- thanks to the use of an inert assistant gas, the samples show total absence of oxides;
- about 65% of the treatments results into the aeronautical specification (thickness of recast layer less than 0.040 mm);
- this work increases understanding of fibre laser trepanning and represents an excellent starting point for future developments.

Acknowledgements The present work was supported by the "Ministero dello Sviluppo Economico" of Italy as part of the PON-FIT research program. Grant No. B01/0707/01-03/X17 is gratefully acknowledged.

This work has been developed within the research line "Statistics, QUAlity and REliability" (SQUARE) of the Joint Laboratory "Interactive DEsign And Simulation" (IDEAS) between the University of Naples Federico II (Italy) and the Fraunhofer Institute for Machine Tools and Forming Technology IWU of Chemnitz (Germany).

The authors are also grateful to *AvioAero* for providing the material adopted in the experimentation.

References

1. Laraia M, Manna M, Cinque G, Di Martino P (2013) A combustor liner cooling system design methodology based on a fluid/structure approach. Appl Therm Eng 60:105–121
2. Cerri G, Giovannelli A, Battisti L, Fedrizzi R (2007) Advances in effusive cooling techniques of gas turbines. Appl Therm Eng 27: 692–698
3. Han JC, Dutta S, Ekkad SV (2000) Gas turbine heat transfer and cooling technology. Taylor & Francis, New York
4. Dhar S, Saini N, Purohit R (2006) A review on laser drilling and its techniques. International Conference on Advances in Mechanical Engineering AME 2006. Fatehgarh Sahib
5. Ashkenasia D, Kaszemeikata T, Muellera N, Dietricha R, Eichlera HJ, Illinga G (2011) Laser trepanning for industrial applications. Phys Procedia 12:323–331
6. Jacobs P (2008) Aerospace applications of precision trepanning. 27th International Congress on Applications of Lasers and Electro-Optics ICALEO 2008. Emecula. CA; USA; 20–23 October 2008. 168–174
7. Sibalija TV, Petronic SZ, Majstorovic VD, Prokic-Cvetkovic R, Milosavljevic A (2011) Multi-response design of Nd:YAG laser drilling of Ni-based superalloy sheets using Taguchi's quality loss function. multivariate statistical methods and artificial intelligence. Int J Adv Manuf Technol 54/5–8:537–552
8. Kling R, Dijoux M, Romoli L, Tantussi F, Sanabria J, Mottay E (2013) Metal micro drilling combining high power femtosecond laser and trepanning head. Proceedings of SPIE. 8608: Article number 86080F
9. Romoli L, Rashed CAA, Fiaschi M (2014) Experimental characterization of the inner surface in micro-drilling of spray holes: a comparison between ultrashort pulsed laser and EDM. Opt Laser Technol 56:35–42
10. Thawari G, Sarin Sundar JK, Sundararajan G, Joshi SV (2005) Influence of process parameters during pulsed Nd:YAG laser cutting of nickel-base superalloys. J Mater Process Technol 170:229–239
11. Dubey AK, Yadava V (2008) Multi-objective optimization of Nd: YAG laser cutting of nickel-based superalloy sheet using orthogonal array with principal component analysis. Opt Lasers Eng 46: 124–132
12. Rao R, Yadava V (2009) Multi-objective optimization of Nd:YAG laser cutting of thin superalloy sheet using grey relational analysis with entropy measurement. Opt Lasers Eng 41:922–930
13. Petronić S, Kovačević G, Milosavljević A, Milosavljević A, Sedmak A (2012) Microstructural changes of Nimonic-263 superalloy caused by laser beam action. Phys Scr T149. Article number 014080
14. Astarita A, Genna S, Leone C, Memola Capece Minutolo F, Paradiso V, Squillace A (2013) Ti-6Al-4V Cutting by 100W fibre laser in both CW and modulated regime. Key Eng Mater 554–557: 1835–1844
15. Biffi CA, Previtali B (2013) Spatter reduction in nanosecond fibre laser drilling using an innovative nozze. Int J Adv Manuf Technol 66:1231–1245
16. Leone C, Genna S, Caggiano A, Tagliaferri V, Molitierno R (2016) Influence of process parameters on kerf geometry and surface roughness in Nd:YAG laser cutting of Al 6061T6 alloy sheet. Int J Adv Manuf Technol 87:2745–2762
17. Lutey AHA, Fortunato A, Ascari A, Carmignato S, Leone C (2015) Laser cutting of lithium iron phosphate battery electrodes: characterization of process efficiency and quality. Opt Laser Technol 65: 164–174
18. Tonshoff HK, Emmelmann C (1989) Laser cutting of advanced ceramics. CIRP Ann Manuf Technol 38:219–222
19. Leone C, Genna S, Tagliaferri V (2014) Fibre laser cutting of CFRP thin sheets by multi-passes scan technique. Opt Lasers Eng 53:43–50.2
20. Genna S, Leone C, Palumbo B, Tagliaferri F (2015) Statistical approach to fiber laser microcutting of NIMONIC® C263

superalloy sheet used in effusion cooling system of aero engines. Proc CIRP 33:520–525
21. Genna S, Tagliaferri F, Leone C, Palumbo B, De Chiara G (2017) Experimental study on fiber laser microcutting of Nimonic 263 superalloy. Proc CIRP 62:281–286
22. Coleman DE, Montgomery DC (1993) A systematic approach to planning for a designed industrial experiment. Technometrics 35(1):1–12
23. Palumbo B, De Chiara G, Marrone R (2008) Innovation via engineering and statistical knowledge integration. In: Erto P (ed) Statistics for innovation, statistical design of continuous product innovation. Springer, Berlin, pp 177–190
24. Leone C, Genna S, Tagliaferri F, Palumbo B, Dix M (2016) Experimental investigation on laser milling of aluminium oxide using a 30 W Q-switched Yb:YAG fiber laser. Opt Laser Technol 76:127–137
25. Tagliaferri F, Dittrich M, Palumbo B (2015) A systematic approach to design of experiments in waterjet machining of high performance ceramics, as chapter of book: management and industrial engineering. Davim: Design of Experiments in Production Engineering, Springer
26. Putz M, Tagliaferri F, Dix M, Wertheim R (2015) Methodology for analysing hybrid cutting processes with thermal assistance. Prod Eng 9:537–549 624, Spring
27. Montgomery DC (2008) Design and analysis of experiments. Wiley, New York
28. Petronić S, Milosavljević A, Radaković Z, Drobnjak P, Grujić I (2010) Analysis of geometrical characteristics of pulsed ND: Yag laser drilled holes in superalloy nimonic 263 sheets. Tehnicki Vjesnik 17(1):61–66
29. Stournaras A, Stavropoulos P, Salonitis K, Chryssolouris G (2009) An investigation of quality in CO_2 laser cutting of aluminium. CIRP J Manuf Sci Technol 2:61–69
30. Adalarasan R, Santhanakumar M, Thileepan S (2016) Selection of optimal machining parameters in pulsed CO2 laser cutting of Al6061/Al2O3 composite using Taguchi-based response surface methodology (T-RSM). Int J Adv Manuf Technol. doi:10.1007/s00170-016-8978-5
31. Kondayya D, Gopala Krishna A (2013) An integrated evolutionary approach for modelling and optimization of laser beam cutting process. Int J Adv Manuf Technol 65/1–4:259–274